Computational insights into the Multi-Diels-Alder reactions of neutral C_{60} and its Li^+ encapsulated analogue: A DFT study

Tamalika Ash[1], Soumadip Banerjee[2], Tanay Debnath[2], and Abhijit Das[2]

[1]Indian Association for the Cultivation of Science
[2]Indian Association for the Cultivation of science

June 11, 2021

Abstract

Diels-Alder cycloaddition reaction is helpful to produce covalent derivatives of fullerene with desirable electronic and physical properties. In the present venture, we have computationally investigated the reactivity of neutral C_{60} and its Li^+ encapsulated derivative towards Multi-Diels-Alder (MDA) reaction with 1,3-butadiene, employing density functional theory (DFT). The computational reports available to date illustrate the functionalization of fullerene surfaces of neutral and encapsulated C_{60} (Ca and Sm) with two butadiene molecules. In this article, we aim to investigate whether more than two butadiene molecules can be attached to the fullerene surface or not. To do so, we have shown that the MDA reaction initiates with the formation of an encounter complex between the mono-functionalized fullerene product and the second butadiene molecule. In this context, two different approaches, namely 'Direct' and 'Alternative' have been considered based on the attachment of the second butadiene, i.e., whether it is attached to the opposite or adjacent position of the first functionalization, which eventually produces the same final product. We have explored the MDA reactions by considering a total of four diene molecules that can be embedded successfully on the fullerene surface, with each reaction step having a high degree of exothermicity, thus making the overall reaction thermodynamically facile. In harmony with the mono- and bis-cycloaddition reactions, for MDA reaction also, the positive impact of Li^+ encapsulation for enhancing the reactivity of fullerene surface towards butadiene attachment is evident from our study. On-the-fly calculations also suggest the bond preference for [6, 6] connectivity than its [6, 5] counterpart, to be the suitable dienophile, just like the mono- and bis-functionalization reported earlier. Overall, the present study will foresee an extensive idea about the detailed mechanism of the MDA reaction on neutral C_{60} and $Li^+@C_{60}$ that could encourage the scientists to perform the aforementioned reaction for other fullerene derivatives in the long run.

1. Introduction:

Since its discovery, buckminsterfullerene[1] has been considered as an important precursor for several chemical compounds which have wide-scale applications [2-7], ranging from material science to biological sciences [8-10]. The functionalization of the fullerene cages including polymeric derivatives has sorted out some of the problems associated with low solubility and miscibility of corresponding C_{60} systems[11].In the past decades, a large number of fullerene derivatives have been synthesized and characterized with desirable applications [12-15], such as photoelectric conversion [16], magnetic resonance imaging [17], cancer therapy[18] and so on. Among the experimental and theoretical methods implemented for fullerene modifications, Diels-Alder cycloaddition reaction[19-23] on the fullerene surface and encapsulation of atom/metal cluster/small molecules into the hollow cage of fullerene [24-27] are drawing great scientific attention. In this aspect, selective encapsulation of fullerene cages is also observed to offer one of the key techniques in their purification [28]. On the I_h-symmetric C_{60}, mainly two kinds of C–C bond connectivity [29] have been observed, namely [6, 6] and [6, 5]. The [6, 6] bond of fullerene (C_{60}) is found to exhibit much higher reactivity towards Diels-Alder reactions with dienes[30, 31] than that of [6, 5] bond[32-35].

In recent decades, extensive studies on the chemical reactivity of endohedral-metallofullerenes (EMFs) have

got a new dimension. The EMFs show enhanced reactivity not only towards Diels-Alder[36] but also to other essential reactions necessary for varied utilization[37]. In this regard, Li^+ encapsulated fullerenes ($Li^+@C_{60}$)[38, 39] are of great interest for both experimentalists as well as theoreticians. According to the studies done by Ueno $et\ al.$ [40], a lesser HOMO-LUMO gap in $Li^+@C_{60}$ compared to neutral C_{60} is the principal reason for facilitating [4+2] cycloaddition reaction, inducing significant changes in the frontier orbitals. As a result, the Diels-Alder reaction of $Li^+@C_{60}$ is 2400-fold faster than neutral C_{60}. However, the effect of counter anion in Li^+-encapsulated C_{60} during the Diels-Alder reaction has also been explored[41].

Cui $et\ al.$ [42] showed the thermodynamic feasibility of cycloaddition reactions between CpH and $Ca^{2+}@C_{60}$ as well as $M^+@C_{60}$ (M = Li, Na, K, Rb, and Cs). Their computational study inferred that encapsulated cations facilitate DA reactions by altering distortion and interaction energies. García-Rodeja and co-workers[43] also explored the influence of varied ion-encapsulation (Li^+, Na^+, K^+, Be^{2+}, Mg^{2+}, Al^{3+}) on the reactivity of the DA reaction between corresponding encapsulated fullerene and 1,3-cyclohexadiene by employing Density Functional Theory (DFT). Osuna $et\ al.$ [44] reported about the modulated reactivity and regio-selectivity in Diels-Alder reaction of noble-gas-encapsulated fullerene systems. Recently, Wu $et\ al.$ [45] observed that [6,5] bond of calcium-encapsulated C_{60} molecule can be successfully activated in the course of DA reaction based on charge transfer from the metal atom to fullerene cage.

After reviewing these earlier reported works, it is quite evident that the investigation of the reactivity of the EMFs in the context of Diels-Alder (DA) reaction is a challenging field of exploration both in terms of the experiment as well as theory. In our previous study[46], we have successfully explored the energetics related to neutral C_{60} as well as mono- and di-cation encapsulated EMFs towards DA reaction with 1,3-butadiene, resulting in mono-functionalized products. But to the best of our knowledge, the reactivity of neutral C_{60} as well as encapsulated C_{60} towards Multi-Diels-Alder (MDA) reaction beyond bis-functionalization[45] is yet to be revealed computationally. Under these circumstances, we are going to investigate the sequential MDA reactions on C_{60} fullerene surface with 1, 3-butadiene computationally by employing DFT. Moreover, in the present venture, we have extended our exploration to the titled reaction procedure for $Li^+@C_{60}$ also to check the effect of metal ion encapsulation on the reactivity of each step of the MDA reaction. In order to get a clear idea about the bond selectivity, both [6, 6] and [6, 5] connectivities on neutral as well as charged EMF surfaces (**Figure 1**) are considered separately for MDA reactions. Overall, our objective is to provide a fundamental understanding of the reactivity of neutral C_{60} towards MDA reactions and to enquire about the effect of Li^+-encapsulation in the reactions, as mentioned earlier.

2. Computational details:

All electronic structure calculations have been carried out using the Gaussian 09[47] suite of the quantum chemistry program. For electronic structure calculations, M06-2X[48] functional in conjunction with 6–31G(d) basis set has been employed. M06-2X functional has been well-established for various theoretical studies such as kinetic and thermodynamic calculations related to Diels-Alder reactions of fullerenes and metallofullerenes[49].This functional is a hybrid meta-GGA functional which was developed by Zhao and Truhlar. It has been found that Quasi-Newton methods are inefficient in finding the transition-state structures (first-order saddle points) between the equilibrium geometries. In this regard, Gaussian incorporates Synchronous Transit-guided Quasi-Newton (STQN) method to search for a maximum along the parabola connecting the reactant and product[50]. A parallel intrinsic reaction coordinate (IRC) calculation [51] has also been performed to confirm whether the transition states connect the right minima or not. Normal-mode analysis has been carried out at the same level of theory to confirm whether the optimized structures are local minima (no imaginary frequency) or transition state geometries (one imaginary frequency).The relative energies of the intermediate adduct (ΔE_A) and transition state (ΔE_{TS}) concerning the separated reactants are defined as:

ΔE_A= E(intermediate adduct)-E(fullerene/metallofullerene)-E(1,3-butadiene);

ΔE_{TS}= E(transition state)-E(fullerene/metallofullerene)-E(1,3-butadiene).

The activation barrier (ΔE_a) is defined as: ΔE_a= ΔE_{TS}-ΔE_A.

2

All energies reported in the article are zero-point-corrected electronic energy obtained at 0 K temperature and 1 atm pressure.

Moreover, kinetics study has also been performed to determine the rate of all Multi-Diels-Alder reactions by employing Transition State Theory (TST) [52, 53]. The entire kinetic study has been performed with The Rate program[54].In this program, the molecular rotations are treated classically and the vibrations are treated quantum mechanically within the harmonic approximation. The rate constant (k) values have been determined for a temperature range of 100 K - 1000 K with 100 K temperature interval, keeping the pressure fixed at 1 atm.

3. Results and Discussion:

In our previous study [46], we have already explored the DA reaction of single 1,3-butadiene moiety with normal fullerene and its mono- and di-encapsulated fullerene derivatives. In the present work, we have extended the study to investigate the MDA reaction on normal fullerene and its mono-encapsulated derivative. The exploration of the Multi-Diels-Alder (MDA) reaction has been commenced by considering the first DA product (first functionalization) and 1, 3-butadiene as the initial reactants. Initially, two different approaches have been adopted for the attachment of the second butadiene on the surface of the first DA product (for both 6-6 and 6-5 connectivity separately). The pictorial diagram of 6-6 and 6-5 bonds are shown in **Figure 1** . The double bond (either 6-6 or 6-5), placed almost opposite to the first functionalization, has been considered for the second butadiene attachment **(Direct Approach)** followed by sequential addition of another two butadiene moieties on the residual 6-6 or 6-5 bonds. In the other approach, designated as the **Alternative Approach** , the double bond adjacent to the first functionalization undergoes a second DA reaction followed by sequential attachment of the other two butadiene molecules on the remaining 6-6 or 6-5 double bonds. The schematic representation of the approaches considered here is depicted in **Scheme 1** . Incidentally, the product formed after two successive DA reactions to the first functionalization, following these two approaches separately, are identical. Each of the six-membered cyclic transition states corresponding to the cyclo-addition is observed to be concerted. The optimized geometries of the TSs for MDA reaction on 6-6 bonds of neutral C_{60} and $Li^+@C_{60}$ and their associated PES diagram are depicted in **Figure 2** and**Figure 3** for the 'Direct' approach and **Figure 4** and**Figure 5** for the 'Alternative' approach, respectively. The graphical representation of [?]E_a on varying the steps of MDA reactions associated with 6-6 bonds for neutral $C_{60}$and $Li^+@C_{60}$ in 'Direct' and 'Alternative' approaches is shown in **Figure 6** and**Figure 7** .

3.1 Direct Approach:

3.1.1 MDA reaction on 6-6 double bond of C_{60}:

The initial adduct, A^1_{6-6O} formed between the 1st DA product (1_{6-6}) and butadiene (diene) molecule is found to be stabilized by 4.2 kcal/mol than the initial reactant pair. The reaction proceeds via the formation of a concerted six-membered transition state (TS^1_{6-6O}) of activation barrier 15.7 kcal/mol in order to form R^1_{6-6O}, which is considered as the second DA product. In R^1_{6-6O}, the associated 6-6 bond length and the newly formed C-C bonds with the butadiene are calculated to be 1.59 and 1.56 Å, respectively. The thermodynamic feasibility of the reaction is evident from its high exothermicity value of -28.2kcal/mol with respect to A^1_{6-6O}. The subsequent adduct (A^2_{6-6O}) formation between $R^1_{6-6O}$and another butadiene molecule is energetically 32.2 kcal/mol more stable than its former adduct complex (A^1_{6-6O}). A^2_{6-6O} undergoes a third DA reaction via TS^2_{6-6O} (**Figure 2**) of barrier height 18.0 kcal/mol to generate R^2_{6-6}. This third functionalized product, R^2_{6-6} is energetically 24.3 kcal/mol more stable than that of A^2_{6-6O} (**Figure 3**). The fourth DA reaction is initiated from the adduct A^3_{6-6}, which is found to be situated at -64.6 kcal/mol in the energy profile diagram. The conversion of A^3_{6-6} to P^4_{6-6} requires an activation barrier of 18.2 kcal/mol (TS^3_{6-6}). Moreover, analyzing the TS geometries of all three DA steps, as depicted in**Figure 2** , it is observed that the bond formation between the diene and fullerene surface occurs almost to the same extent, suggesting the process to be synchronous in nature.

In short, we have explored the incorporation of a total of four 1, 3-butadiene molecules on the surface of neutral C_{60} via the MDA functionalization process, considering 6-6 bond connectivity to be the dienophile.

Moreover, a gradual rise in the stabilization energy due to consecutive attachment of butadiene molecules to 1_{6-6} is noticeable. The final product, P^4_{6-6} is found to be-88.5 kcal/mol downhill than the starting reactant, 1_{6-6}, suggesting the MDA functionalization procedure to be highly thermodynamically facile.

3.1.2 MDA reaction on 6-6 double bond of Li$^+$@C$_{60}$:

To check the effect of Li$^+$ encapsulation on MDA reaction, we have explored all three steps associated with the MDA reaction on 1_{6-6L}. It has been well-established that the encapsulation of Li$^+$ enhances the reactivity of 6-6 double bond of fullerene towards DA reactions and yields mono-functionalized fullerene as the first DA product[46]. Here, we intend to examine whether the effectiveness of Li$^+$ encapsulation during MDA reaction associated with the 6-6 double bonds persists or not. The second DA reaction originated from A^1_{6-6OL} (**Figure 3**) is observed to be 7.8 kcal/mol more stable than the initial reactants. The activation barrier associated with the conversion of A^1_{6-6OL} to R^1_{6-6OL} via TS^1_{6-6OL} is found to be 11.7 kcal/mol, which is 4.0 kcal/mol lower in energy than its neutral counterpart. The enthalpy change involves in R^1_{6-6OL} formation is -29.0 kcal/mol, which is ˜1.0 kcal/mol lower than its R^1_{6-6O} fabrication. So, it can be articulated that Li$^+$-encapsulation successfully enhances the reactivity of encapsulated fullerene towards the second DA reaction by reducing the activation barrier. As evident from **Figure 3**, the third DA reaction is initiated from A^2_{6-6OL}, which is placed at -44.9 kcal/mol on the PES. The activation barrier associated with TS^2_{6-6OL} (**Figure 2**) corresponding to R^2_{6-6L} formation is found to be 3.6 kcal/mol lower than the neutral C$_{60}$ analogue. The exothermic nature of this step is also noted from the associated enthalpy change of -26.9 kcal/mol with respect to A^2_{6-6OL}, which is 2.4 kcal/mol lower than that of neutral C$_{60}$. For the fourth DA reaction, the adduct, A^3_{6-6L} (stabilized at-76.9 kcal/mol on the PES) generates P^4_{6-6L} through a transition state, TS^3_{6-6L}, with a barrier height 14.6 kcal/mol. The end product, P^4_{6-6L} is -101.8kcal/mol downhill than the starting reactant 1_{6-6L}, indicating the entire process to be thermodynamically feasible in nature. In this case, all three steps are also identified as synchronous processes as the newly formed C-C bonds between the fullerene surface and diene in the TSs are calculated to be nearly equal in length.

Thus, from our computational analysis, it is evident that for Li$^+$@C$_{60}$, all three steps of MDA reactions are more likely to occur both kinetically as well as thermodynamically due to reduced activation barrier and higher exothermicity than its neutral counterpart. So, it can be inferred that Li$^+$ encapsulation significantly affects the reactivity in each step of the 6-6 MDA reaction.

3.1.3 MDA reaction on 6-5 double bond of C$_{60}$:

The initial adduct, A^1_{6-5O} formed between the first DA product (1_{6-5}) and butadiene molecule is found to be stabilized by -4.2kcal/mol than its initial counterparts. The conversion of A^1_{6-5O} to R^1_{6-5O} involves an activation height of 26.4 kcal/mol (TS^1_{6-5O}), which is 10.7kcal/mol higher than TS^1_{6-6O}. Though the thermodynamic feasibility of the reaction is evident from the exothermicity value of 9.4 kcal/mol, the resultant product, R^1_{6-5O} is found to be 18.8kcal/mol less stable than its 6-6 fabrication. The subsequent adduct for third functionalization, A^2_{6-5O} is 13.8kcal/mol more stable than A^1_{6-5O}. During the third DA reaction, R^2_{6-5} formation needs activation energy of 23.2 kcal/mol (TS^2_{6-5O}), which is nearly 3.0 kcal/mol less than its former step, but 5.2 kcal/molhigher than its corresponding 6-6 analogue. The adduct, A^3_{6-5} placed at -35.8 kcal/mol on PES, gives rise to tetra-functionalized product, P^4_{6-5} via a six-member transition state, TS^3_{6-5} of activation barrier 23.5 kcal/mol. The thermodynamic feasibility of successive butadiene attachment to 1_{6-5} is clearly evident from the negative enthalpy values associated with all three steps of the 6-5 MDA reaction. Moreover, the net energy release for the overall reaction procedure is calculated to be -48.9 kcal/mol.

Similar to its 6-6 analogue, the addition of a second diene molecule to the 6-5 bond of fullerene surface is observed to be a synchronous process. Nevertheless, unlike the 6-6 one, the asynchronicity arises in the case of third and fourth DA reactions as the difference of lengths between the two newly formed C-C bonds in the TS is nearly 0.4 Å (**Figure S1**).

3.1.4 MDA reaction on 6-5 double bond of Li$^+$@C$_{60}$:

In this section, we have spelled out the effect of Li$^+$encapsulation on 6-5 MDA reactions. The formation

4

energy of the initial adduct, $A^1_{6\text{-}5OL}$ (**Figure S2**) is nearly 2.0 kcal/mol lower than that of neutral C_{60} for this particular step. The activation barrier ($TS^1_{6\text{-}5OL}$) and enthalpy change for $R^1_{6\text{-}5OL}$ formation are 20.9 and 12.9 kcal/mol, respectively, which are 5.5 and 3.5 kcal/mol lower and higher than its uncharged counterpart. The third DA reaction has been initiated from $A^2_{6\text{-}5OL}$, which is 5.5 kcal/mol more stable than $R^1_{6\text{-}5OL}$. The transition state, $TS^2_{6\text{-}5OL}$(**Figure S1**), necessary for $R^2_{6\text{-}5L}$formation, is 10.5 kcal/mol downhill than its neutral analogue. The exothermic nature of this step is also noted from its corresponding enthalpy change (-17.5 kcal/mol). The adduct complex, $A^3_{6\text{-}5L}$ necessary for the fourth functionalization is energetically 4.4 kcal/mol more stable than $R^2_{6\text{-}5OL}$.The activation barrier ($TS^3_{6\text{-}5L}$) associated with tetra-substituted $P^4_{5\text{-}6L}$ formation is nearly 9.0 kcal/mol, lesser than its neutral analogue. The net exothermicity corresponds to the overall reaction procedure is -65.5 kcal/mol.

Similar to the neutral C_{60}, for $Li^+@C_{60}$ also, the second DA reaction is a synchronous process. However, both the third and fourth DA reactions exhibit greater asynchronicity than the neutral analogues as the difference of lengths between the two newly formed C-C bonds in the TS becomes more than 1.0 Å.

Thus, from our computational analysis, it is evident that each step of sequential 6-5 MDA reactions on $Li^+@C_{60}$ is kinetically more feasible and thermodynamically more attainable than neutral C_{60}, just like its 6-6 counterparts.

3.2 Alternative Approach:

3.2.1 MDA reaction on 6-6 double bond of C_{60}:

As evident from **Figure 5** , the stability of the first DA adduct for the alternative approach, i.e., $A^1_{6\text{-}6S}$ (-4.1 kcal/mol) is comparable with $A^1_{6\text{-}6O}$. The activation barrier involved for $R^1_{6\text{-}6S}$ formation via $TS^1_{6\text{-}6S}$ is calculated to be 17.3 kcal/mol, which is only 1.6 kcal/mol higher than the corresponding direct pathway. Thus, we can say that a fruitful second DA reaction can be done by placing the butadiene molecule not only at the opposite of the first functionalization but also at the adjacent position. The addition of third butadiene molecule can be done either opposite to the first functionalization or second functionalization in $R^1_{6\text{-}6S}$, but eventually both generate the same tri-functionalized product ($R^2_{6\text{-}6}$) obtained in the 'Direct' approach. The associated adduct complex, $A^2_{6\text{-}6S}$ is placed at -36.5 kcal/mol on the energy profile diagram, which is energetically comparable with $A^2_{6\text{-}6O}$. The transition state $TS^2_{6\text{-}6S}$ (**Figure 4**) associated with the formation of $R^2_{6\text{-}6}$ requires a barrier height of 18.0 kcal/mol, which is exactly the same as the direct one. Similar to the second functionalization, the third functionalization is also highly exothermic as the associated product, $R^2_{6\text{-}6}$ is -24.2 kcal/mol more stable than $A^2_{6\text{-}6S}$. For the attachment of the fourth butadiene, it will precisely follow similar pathway proposed for the 'Direct' approach.

Like 'Direct' approach, for the 'Alternative' approach also, as shown in**Figure 4** , all three DA reactions are synchronous processes as the vibrations associated with the new C-C bonds occur to an equal extent in the TS geometry.

3.2.2 MDA reaction on 6-6 double bond of $Li^+@C_{60}$:

The preliminary adduct complex, $A^1_{6\text{-}6SL}$ (7.7 kcal/mol) is identified as equally stable like its direct counterpart. As depicted in**Figure 5** , the activation barrier corresponding to the conversion of $A^1_{6\text{-}6SL}$ to $R^1_{6\text{-}6SL}$ via $TS^1_{6\text{-}6SL}$ is lowered by 4.2 kcal/mol compared to its neutral counterpart. The associated enthalpy change (-32.1 kcal/mol) indicates that the second functionalization on Li^+-encapsulated fullerene via alternative way is also thermodynamically feasible. In the third DA reaction, the barrier height ($TS^1_{6\text{-}6SL}$) corresponding to $R^2_{6\text{-}6L}$formation is 14.1 kcal/mol, which is almost comparable to its 'Direct' analogue. The exothermic nature of the third DA reaction is also noted from the associated enthalpy change (-27.3 kcal/mol). Similar to the neutral C_{60} analogue, for $Li^+@C_{60}$ also, the addition of fourth butadiene molecule will be obtained in a similar way to that of the 'Direct' one. Like the neutral C_{60} fabrication, for $Li^+@C_{60}$also, all three DA steps are synchronous as the maximum difference of bond length between the two C-C bonds forming between the diene moiety and fullerene surface in the TS is 0.026 Å.

3.2.3 MDA reaction on 6-5 double bond of C_{60}:

As shown in **Figure S4** , for 6-5 also, the energy release associated with A^1_{6-5S} formation (-4.3 kcal/mol) is noticed to be comparable enough with its 'Direct' counterpart. The transition state (TS^1_{6-5S}) for R^1_{6-5S} formation requires nearly 10.8 kcal/mol higher energy than its 6-6 analogue. The enthalpy change associated with R^1_{5-6S} production is observed to be -13.6 kcal/mol, inferring the thermodynamic viability of the second DA reaction through the 'Alternative' approach. In the third DA reaction, A^2_{6-5S} needs 27.4 kcal/mol activation energy (TS^1_{6-5S}) for R^2_{6-5} formation, which is not only 9.4 kcal/mol higher than its 6-6 counterpart but also 4.2 kcal/mol higher than the corresponding barrier obtained in the 'Direct' approach. This reaction step is also exothermic, just like the previous DA steps, with the associated reaction enthalpy value of -10.7 kcal/mol. For the fourth DA reaction, the pathway will be exactly identical with the one established for 6-5 bond in the 'Direct' approach.

Similar to the 'Direct' approach, in this case also, asynchronicity arises in the third and fourth TSs as the difference of C-C bond lengths is 0.2 and 0.4 Å, respectively (**Figure S3**).

3.2.4 MDA reaction on 6-5 double bond of $Li^+@C_{60}$:

The energy release associated with A^1_{6-5SL} formation is calculated to be 6.6 kcal/mol, which is comparable to its 'Direct' counterpart (**Figure S4**).The barrier height (TS^1_{6-5SL}) corresponding to R^1_{5-6SL} formation is 6.0 kcal/mol lower than its neutral counterpart. The associated enthalpy change (-19.8 kcal/mol) suggests the second functionalization on $1_{6-5L}$to be exothermic in nature and thus thermodynamically facile. The third DA reaction has been initiated from A^2_{6-5SL}, which eventually generates R^2_{6-5L}.The associated activation height (TS^2_{6-5SL}) is noted to be 8.2 kcal/mol lower than its uncharged analogue. The exothermic nature of the third DA step is also noted from its corresponding enthalpy change (-12.9 kcal/mol). The fourth functionalization follows a similar mechanism to the one proposed for the 'Direct' pathway.

Unlike the 'Direct'pathway, the asynchronicity arises in the second DA reaction and becomes more prominent in the third and fourth DA reactions. The difference of lengths between the two newly forming C-C bonds in the TS is 0.6 Å for the second TS, which enhances to ~ 1.0 Å for both third and fourth TSs.

In short, it can be easily articulated that Li^+encapsulation does affect the reactivity in each step of 6-6 as well as 6-5 MDA reaction irrespective of the approaches considered, i.e., whether 'Direct' or 'Alternative' approach.

3.3 TST Calculation:

From TST calculation, shown in **Table S1,** it is evident that for neutral C_{60}, for both the 'Direct' as well as 'Alternative' approaches, each step of the 6-6 MDA reaction is kinetically feasible at 400 K. The second DA step via 'Direct' approach is observed to be 10 times faster than the 'Alternative' approach. In harmony with the activation barrier calculation, the rate constants for the third functionalization are calculated to be comparable enough irrespective of the approaches. The rate constant (k) for the fourth DA reaction is observed to be 1.48 sec^{-1} at 400 K. However, the change in magnitudes of rate constants for the 6-6 MDA reaction of $Li^+@C_{60}$ is in accordance with the diminished activation barrier for each step compared to its neutral analogue. From **Table S2** , it is apparent that each step of the MDA reaction via 'Direct' as well as 'Alternative' approaches is kinetically achievable in between 300 K - 400 K. However, the associated rate constants for both second and third DA reactions in 'Direct' pathway are 10 times faster than the respective 'Alternative' pathway at 300 K. The value of k for the final functionalization step at 300 K is calculated to be 0.89 sec^{-1}.

The kinetic study also infers that a relatively higher temperature is required for the kinetic attainment of 6-5 MDA reaction than their 6-6 counterpart for both neutral C_{60} as well as $Li^+@C_{60}$ (**Table S3** and**Table S4**). The magnitudes of rate constants suggest that temperature range 500 K-600 K is suitable for 6-5 MDA reaction in the absence of Li^+, which eventually changes to 400 K-500 K due to Li^+ encapsulation.

4. Conclusion:

In this article, the MDA reaction on neutral C_{60} has been computationally explored employing DFT where

6-6 as well as 6-5 bonds are considered. In addition, we have also investigated the effect of Li^+ encapsulation on the energetics of each step of the MDA reaction. The consecutive attachments of butadiene molecules on neutral C_{60} and $Li^+@C_{60}$ commences with the formation of a 1:1 precursor complex between the mono-functionalized fullerene product and a butadiene molecule. In this regard, two possible approaches ('Direct' and 'Alternative') have been considered separately, leading to the same tri-functionalized fullerene product after two consecutive additions of butadiene molecules. We have explored the MDA reaction considering the attachment of a total of four diene molecules on the surface of the fullerene cage. Each reaction step shows a high degree of exothermicity, suggesting that the entire reaction is thermodynamically feasible. However, from the PES diagrams, it is evident that Li^+ encapsulation makes a positive impact by decreasing the activation barrier and increasing the reaction enthalpy than their neutral counterparts. Thus, we can conclude that MDA reactions become thermodynamically more facile due to Li^+ confinement in the C_{60} cage. Moreover, in the MDA procedure also, the persistence of bond selectivity, i.e., the higher reactivity of [6, 6] bonds over [6, 5], just like mono and bis-functionalization, has been noticed for both C_{60} and $Li^+@C_{60}$. In a nutshell, the exploration of all possible steps related to MDA reaction on neutral as well as Li^+ endohedral C_{60} will motivate the researchers to investigate more complex reactions related to fullerene chemistry for varied applications.

Acknowledgement

Supporting Information

Values of rate constants (k) obtained from TST calculation (**Table S1** to **Table S4**); Optimized geometries of the TSs for MDA reaction on 6-5 bonds of neutral C_{60} and $Li^+@C_{60}$ and their associated PES diagram for 'Direct' approach (**Figure S1** and **Figure S2**); Optimized geometries of the TSs for MDA reaction on 6-5 bonds of neutral C_{60} and $Li^+@C_{60}$ and their associated PES diagram for 'Alternative' approach (**Figure S3** and **Figure S4**); Graphical representation of [?]E_a on varying the steps of MDA reactions associated with 6-5 bonds for both neutral C_{60} and $Li^+@C_{60}$ in 'Direct' and 'Alternative' approaches (**Figure S5** and **Figure S6**); xyz coordinates of all reactants, TSs and products involved in the entire MDA reaction.

Reference:

[1] Kroto, H. W.; Heath, J. R.; O'Brien, S. C.; Curl, R. F.; Smalley, R. E. Nature 1985, 318, 162-163.

[2] Buntar, V.; Weber, H. W. Superconductor Science and Technology 1996, 9, 599-615.

[3] Cami, J.; Bernard-Salas, J.; Peeters, E.; Malek, S. E. Science 2010, 329, 1180.

[4] Campbell, E. K.; Holz, M.; Gerlich, D.; Maier, J. P. Nature 2015, 523, 322-323.

[5] Deibel, C.; Dyakonov, V. Reports on Progress in Physics 2010, 73, 096401.

[6] Foing, B. H.; Ehrenfreund, P. Nature 1994, 369, 296-298.

[7] Fulara, J.; Jakobi, M.; Maier, J. P. Chemical Physics Letters 1993, 211, 227-234.

[8] Goodarzi, S.; Da Ros, T.; Conde, J.; Sefat, F.; Mozafari, M. Materials Today 2017, 20, 460-480.

[9] Speltini, A.; Merli, D.; Profumo, A. Analytica Chimica Acta 2013, 783, 1-16.

[10] Semenov, K. N.; Charykov, N. A.; Postnov, V. N.; Sharoyko, V. V.; Vorotyntsev, I. V.; Galagudza, M. M.; Murin, I. V. Progress in Solid State Chemistry 2016, 44, 59-74.

[11] Diniakhmetova, D. R.; Friesen, A. K.; Kolesov, S. V. 2020, 120, e26335.

[12] Billups, W. E. Journal of the American Chemical Society 2005, 127, 11876-11876.

[13] Lin, H.-S.; Matsuo, Y. Chemical Communications 2018, 54, 11244-11259.

[14] Martin, N. Chemical Communications 2006, 2093-2104.

[15] Thilgen, C.; Diederich, F. Chemical Reviews 2006, 106, 5049-5135.

[16] He, Y.; Li, Y. Physical Chemistry Chemical Physics 2011, 13, 1970-1983.

[17] Bolskar, R. D. Nanomedicine 2008, 3, 201-213.

[18] Wang, T.; Wang, C. 2019, 15, 1901522.

[19] Hatzimarinaki, M.; Vassilikogiannakis, G.; Orfanopoulos, M. Tetrahedron Letters 2000, 41, 4667-4670.

[20] Pla, P.; Wang, Y.; Alcami, M. Physical Chemistry Chemical Physics 2020, 22, 8846-8852.

[21] Śliwa, W. Fullerene Science and Technology 1997, 5, 1133-1175.

[22] Vassilikogiannakis, G.; Hatzimarinaki, M.; Orfanopoulos, M. The Journal of Organic Chemistry 2000, 65, 8180-8187.

[23] Vassilikogiannakis, G.; Orfanopoulos, M. Journal of the American Chemical Society 1997, 119, 7394-7395.

[24] Aoyagi, S.; Nishibori, E.; Sawa, H.; Sugimoto, K.; Takata, M.; Miyata, Y.; Kitaura, R.; Shinohara, H.; Okada, H.; Sakai, T.; Ono, Y.; Kawachi, K.; Yokoo, K.; Ono, S.; Omote, K.; Kasama, Y.; Ishikawa, S.; Komuro, T.; Tobita, H. Nature Chemistry 2010, 2, 678-683.

[25] Vidal, S.; Izquierdo, M.; Alom, S.; Garcia-Borràs, M.; Filippone, S.; Osuna, S.; Solà, M.; Whitby, R. J.; Martín, N. Chemical Communications 2017, 53, 10993-10996.

[26] Maroto, E. E.; Mateos, J.; Garcia-Borràs, M.; Osuna, S.; Filippone, S.; Herranz, M. Á.; Murata, Y.; Solà, M.; Martín, N. Journal of the American Chemical Society 2015, 137, 1190-1197.

[27] Bologna, F.; Mattioli, E. J.; Bottoni, A.; Zerbetto, F.; Calvaresi, M. ACS Omega 2018, 3, 13782-13789.

[28] Camacho Gonzalez, J.; Mondal, S.; Ocayo, F.; Guajardo-Maturana, R.; Muñoz-Castro, A. 2020, 120, e26080.

[29] Kroto, H. W. Nature 1987, 329, 529-531.

[30] Kawakami, H.; Okada, H.; Matsuo, Y. Organic Letters 2013, 15, 4466-4469.

[31] Ueno, H.; Kawakami, H.; Nakagawa, K.; Okada, H.; Ikuma, N.; Aoyagi, S.; Kokubo, K.; Matsuo, Y.; Oshima, T. Journal of the American Chemical Society 2014, 136, 11162-11167.

[32] Tran, C.; Sakai, H.; Kawashima, Y.; Ohkubo, K.; Fukuzumi, S.; Murata, H. Organic Electronics 2017, 45.

[33] Supur, M.; Kawashima, Y.; Ohkubo, K.; Sakai, H.; Hasobe, T.; Fukuzumi, S. Physical Chemistry Chemical Physics 2015, 17, 15732-15738.

[34] Ohkubo, K.; Kawashima, Y.; Sakai, H.; Hasobe, T.; Fukuzumi, S. Chemical Communications 2013, 49, 4474-4476.

[35] Fukuzumi, S.; Ohkubo, K. Dalton Transactions 2013, 42, 15846-15858.

[36] Karimi, J.; Izadyar, M.; Nakhaeipour, A. Structural Chemistry 2020, 31, 1821-1829.

[37] Lu, X.; Bao, L.; Akasaka, T.; Nagase, S. Chemical Communications 2014, 50, 14701-14715.

[38] Aoyagi, S.; Sado, Y.; Nishibori, E.; Sawa, H.; Okada, H.; Tobita, H.; Kasama, Y.; Kitaura, R.; Shinohara, H. 2012, 51, 3377-3381.

[39] Aoyagi, S.; Tokumitu, A.; Sugimoto, K.; Okada, H.; Hoshino, N.; Akutagawa, T. Journal of the Physical Society of Japan 2016, 85, 094605.

[40] Ueno, H.; Nishihara, T.; Segawa, Y.; Itami, K. 2015, 54, 3707-3711.

[41] Zhang, D.; Li, H.; Wang, H.; Li, L. 2016, 116, 1846-1850.

[42] Cui, C.-X.; Liu, Y.-J. The Journal of Physical Chemistry A 2015, 119, 3098-3106.

[43] García-Rodeja, Y.; Solà, M.; Bickelhaupt, F. M.; Fernández, I. 2017, 23, 11030-11036.

[44] Osuna, S.; Swart, M.; Solà, M. 2009, 15, 13111-13123.

[45] Wu, Y.; Jiang, Y.; Deng, J.; Wang, Z. Physical Chemistry Chemical Physics 2020, 22, 24249-24256.

[46] Debnath, T.; Ash, T.; Saha, J. K.; Das, A. K. 2017, 2, 4039-4053.

[47] Frisch MJ, Trucks GW, Schlegel HB, Scuseria GE, Robb MA, Cheeseman JR, Scalmani G, Barone V, Mennucci B, PeterssonGA, Nakatsuji H, Caricato M, Li X, Hratchian HP,Izmaylov AF, Bloino J, Zheng G, Sonnenberg JL, Hada M,Ehara M, Toyota K, Fukuda R, Hasegawa J, Ishida M,Nakajima T, Honda Y, Kitao O, Nakai H, Vreven T,Montgomery Jr JA, Peralta JE, Ogliaro F, Bearpark MJ, Heyd J,Brothers EN, Kudin KN, Staroverov VN, Kobayashi R,Normand J, Raghavachari K, Rendell AP, Burant JC,Iyengar SS, Tomasi J, Cossi M, Rega N, Millam NJ, Klene M,Knox JE, Cross JB, Bakken V, Adamo C, Jaramillo J,GompertsR Stratmann RE, Yazyev O, Austin AJ, Cammi R,Pomelli C, Ochterski JW, Martin RL, Morokuma K,Zakrzewski VG, VothGA, Salvador P, Dannenberg JJ,Dapprich S, Daniels AD, Farkas \euroO, Foresman JB, Ortiz JV,Cioslowski J, Fox DJ. Gaussian 09. Wallingford, CT: Revision D.01. Inc.; 2013.

[48] Zhao, Y.; Truhlar, D. G. Theoretical Chemistry Accounts 2008, 120, 215-241.

[49] Sato, S.; Maeda, Y.; Guo, J.-D.; Yamada, M.; Mizorogi, N.; Nagase, S.; Akasaka, T. Journal of the American Chemical Society 2013, 135, 5582-5587.

[50] Peng, C.; Bernhard Schlegel, H. 1993, 33, 449-454.

[51] Gonzalez, C.; Schlegel, H. B. The Journal of Physical Chemistry 1990, 94, 5523-5527.

[52] Truhlar, D. G.; Garrett, B. C.; Klippenstein, S. J. The Journal of Physical Chemistry 1996, 100, 12771-12800.

[53] Evans, M. G.; Polanyi, M. Transactions of the Faraday Society 1935, 31, 875-894.

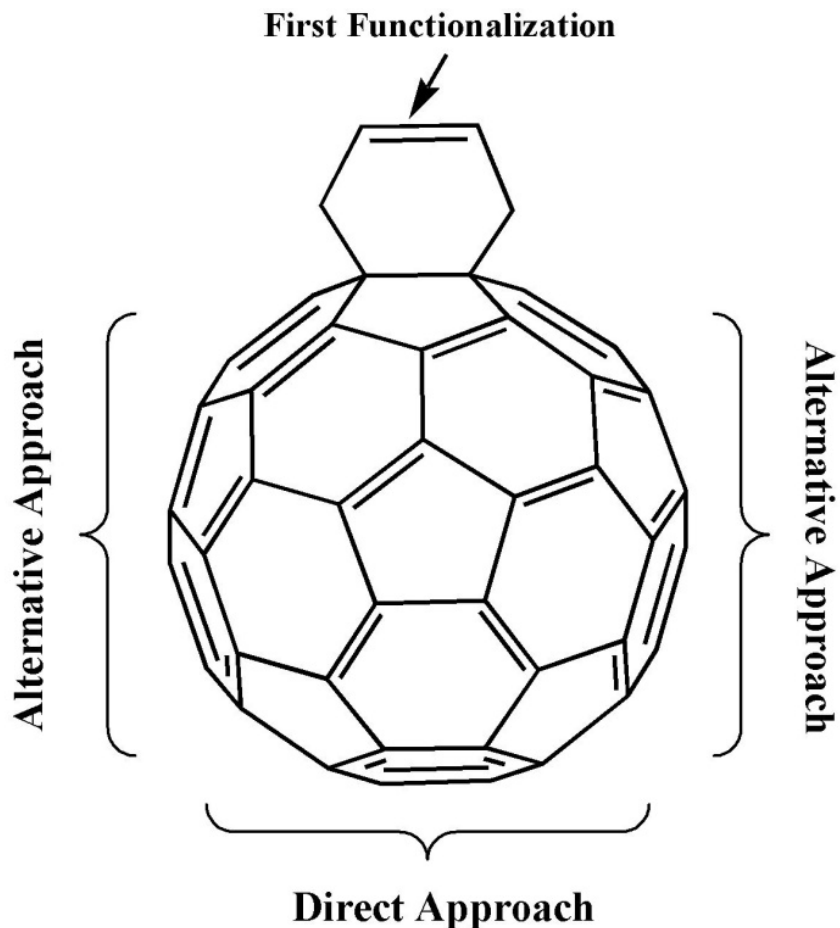[54] Duncan, W. T.; Bell, R. L.; Truong, T. N. 1998, 19, 1039-1052.

First Functionalization

Alternative Approach

Alternative Approach

Direct Approach

FIGURE LEGENDS

FIGURE 1 The [6, 6] and [6, 5] bond connectivity in fullerene analogues.

FIGURE 2 Optimized geometries of transition states involved in the Multi-Diels-Alder reaction associated with the 6-6 bonds of (A) neutral C_{60} and (B) $Li^+@C_{60}$ in 'Direct' approach. All bond lengths are in Angstrom (Å) unit.

FIGURE 3 Potential energy surface (PES) for the Multi-Diels-Alder reaction associated with the 6-6 bonds of neutral C_{60} and $Li^+@C_{60}$ in 'Direct' approach at M06-2X/6-31G(d) level. Relative energy values are given in kcal/mol.

FIGURE 4 Optimized geometries of transition states involved in the Multi-Diels-Alder reaction associated with the 6-6 bonds of (A) neutral C_{60} and (B) $Li^+@C_{60}$ in 'Alternative' approach. All bond lengths are in Angstrom (Å) unit.

FIGURE 5 Potential energy surface (PES) for the Multi-Diels-Alder reaction associated with the 6-6 bonds of neutral C_{60} and $Li^+@C_{60}$ in 'Alternative' approach at M06-2X/6-31G(d) level. Relative energy values are given in kcal/mol.

FIGURE 6 Graphical representation of [?]Ea on varying the steps of MDA reactions associated with 6-6 bonds in 'Direct' approach for both neutral C_{60} and $Li^+@C_{60}$.

10

FIGURE 7 Graphical representation of [?]Ea on varying the steps of MDA reactions associated with 6-6 bonds in 'Alternative' approach for both neutral C_{60} and $Li^+@C_{60}$.
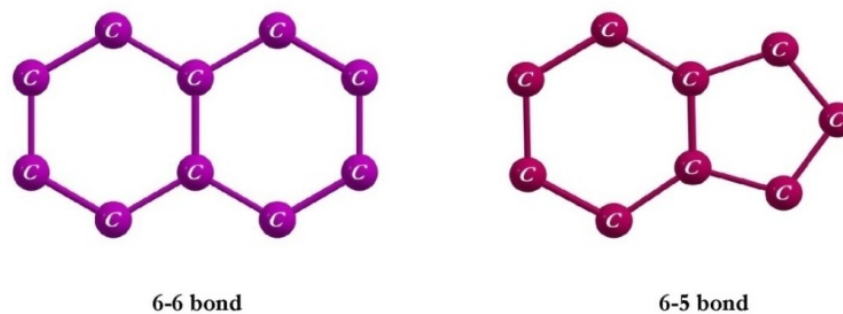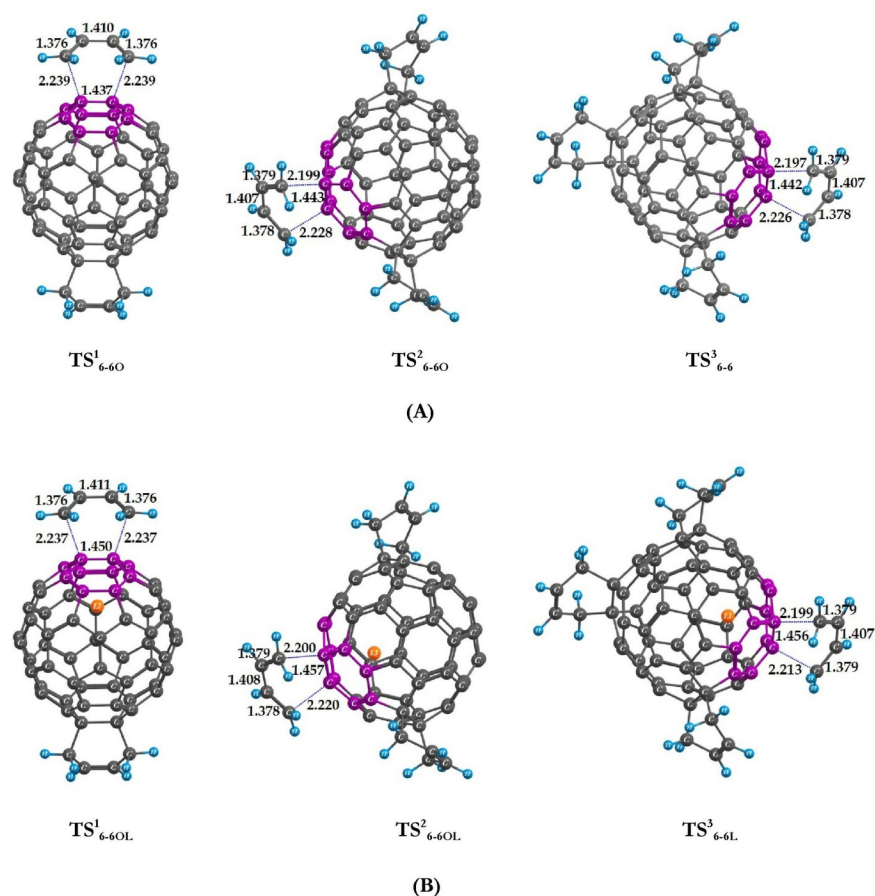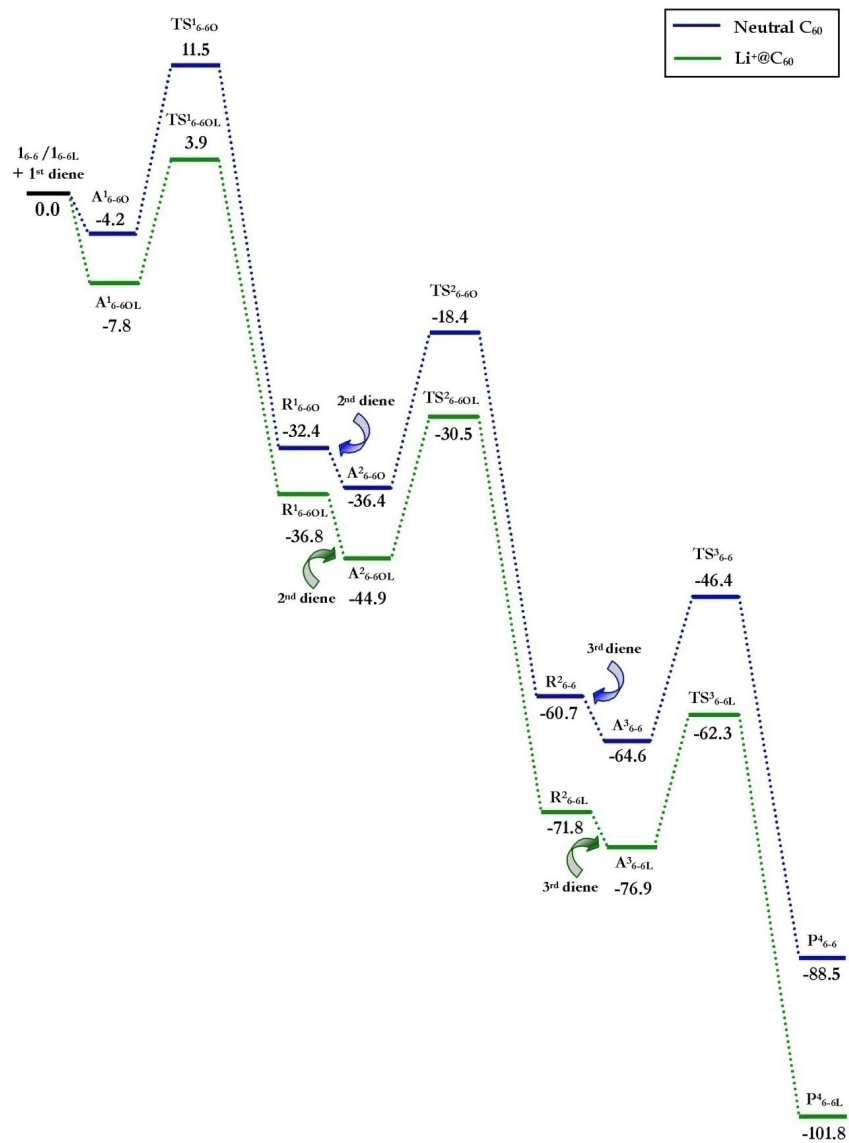

6-6 bond   **6-5 bond**

FIGURE 1 The [6, 6] and [6, 5] bond connectivity in fullerene analogues.

TS^1_{6-6O} TS^2_{6-6O} TS^3_{6-6}

(A)

TS^1_{6-6OL} TS^2_{6-6OL} TS^3_{6-6L}

(B)

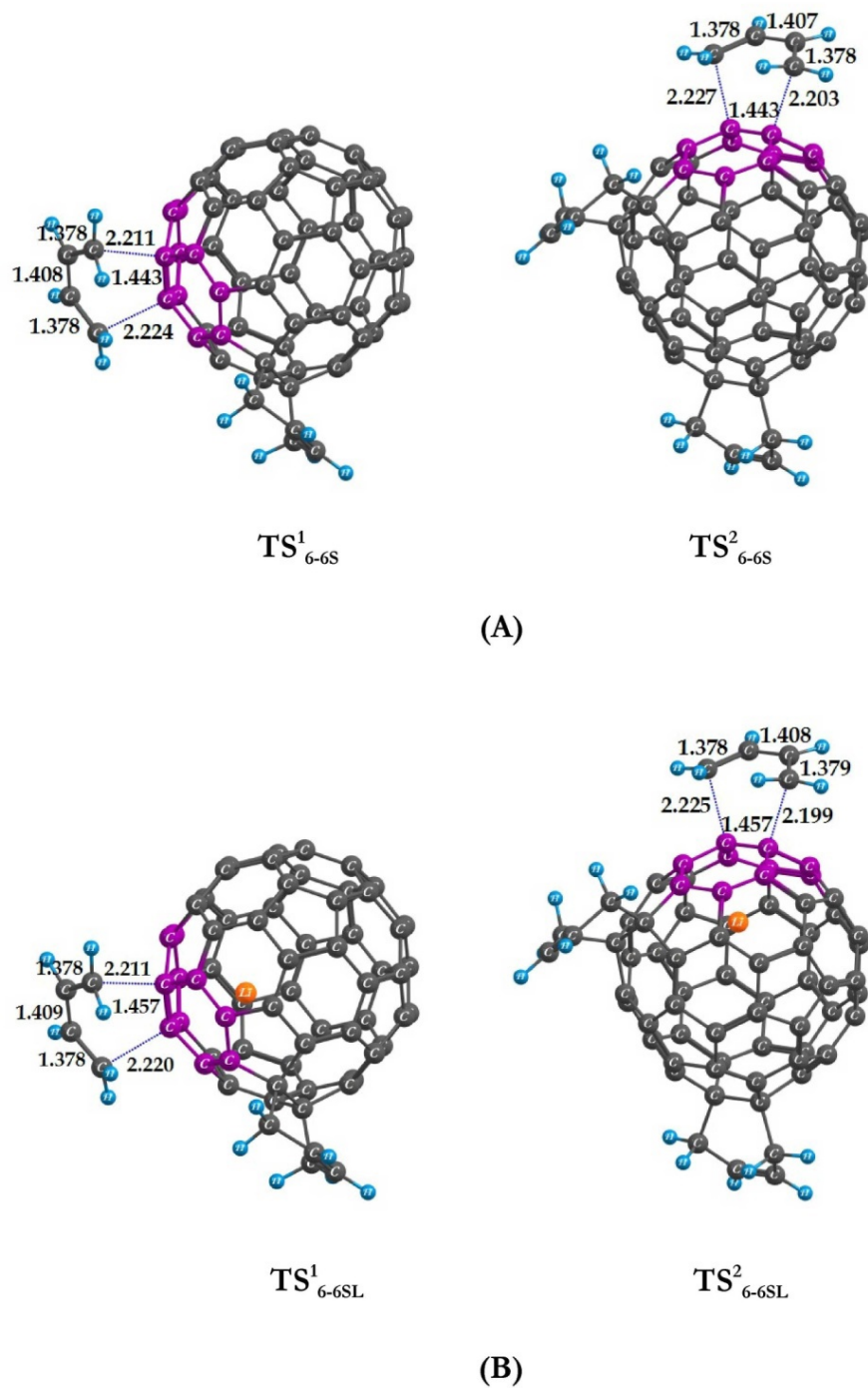**FIGURE 2** Optimized geometries of transition states involved in the Multi-Diels-Alder reaction associated with the 6-6 bonds of (A) neutral C_{60} and (B) $Li^+@C_{60}$ in 'Direct' approach. All bond lengths are in Angstrom (Å) unit.

11

FIGURE 3 Potential energy surface (PES) for the Multi-Diels-Alder reaction associated with the 6-6 bonds of neutral C_{60} and $Li^+@C_{60}$ in 'Direct' approach at M06-2X/6-31G(d) level. Relative energy values are given in kcal/mol.

TS$^1_{6-6S}$ **TS**$^2_{6-6S}$

(A)

TS$^1_{6-6SL}$ **TS**$^2_{6-6SL}$

(B)

FIGURE 4 Optimized geometries of transition states involved in the Multi-Diels-Alder reaction associated with the 6-6 bonds of (A) neutral C_{60} and (B) $Li^+@C_{60}$ in 'Alternative' approach. All bond lengths are in Angstrom (Å) unit.
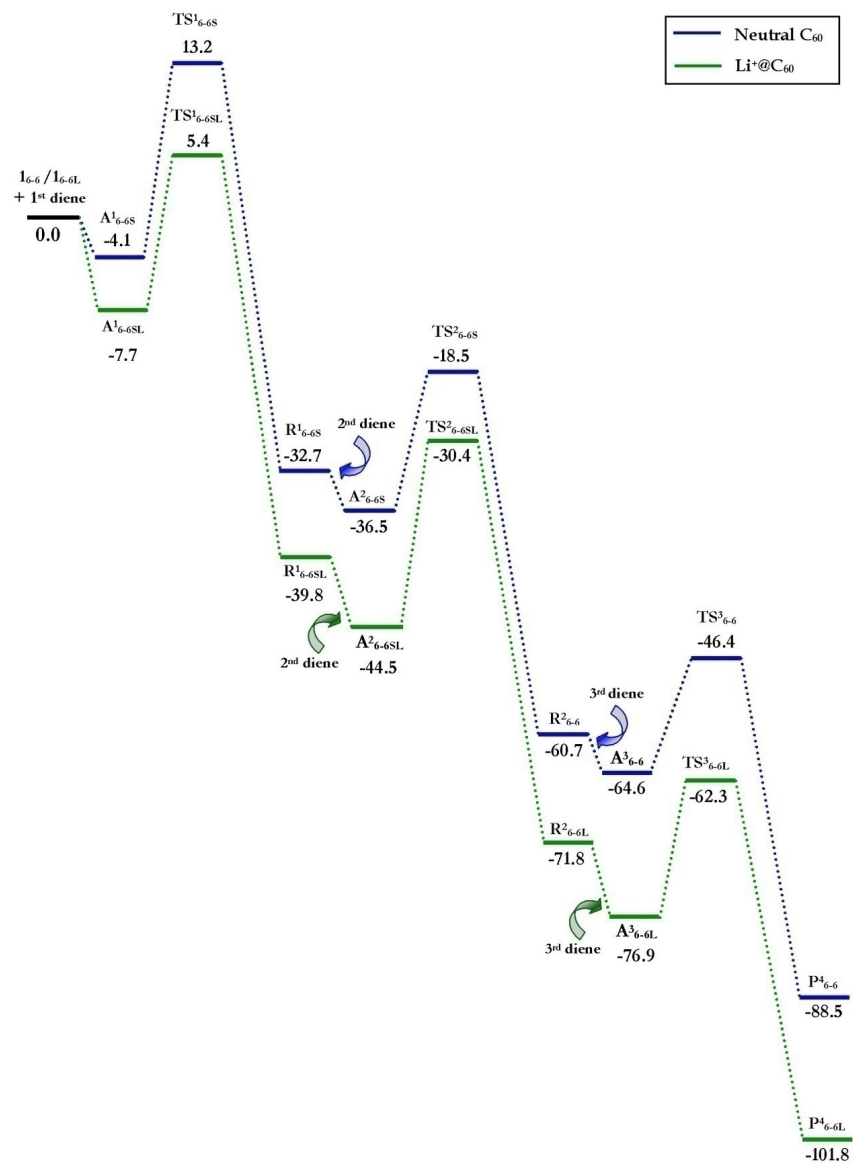
13

FIGURE 5 Potential energy surface (PES) for the Multi-Diels-Alder reaction associated with the 6-6 bonds of neutral C_{60} and $Li^+@C_{60}$ in 'Alternative' approach at M06-2X/6-31G(d) level. Relative energy values are given in kcal/mol.
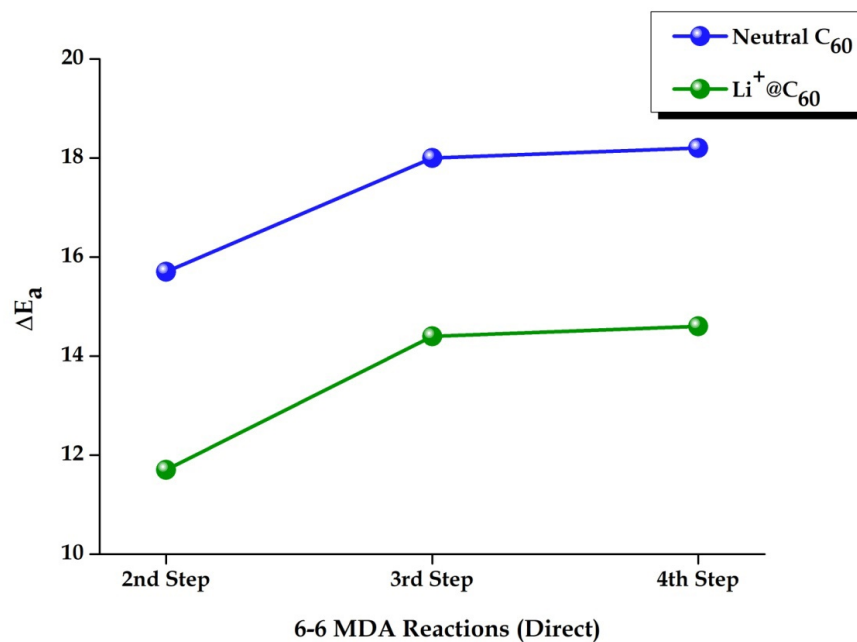
FIGURE 6 Graphical representation of $[?]E_a$ on varying the steps of MDA reactions associated with 6-6 bonds in 'Direct' approach for both neutral C_{60} and $Li^+@C_{60}$.
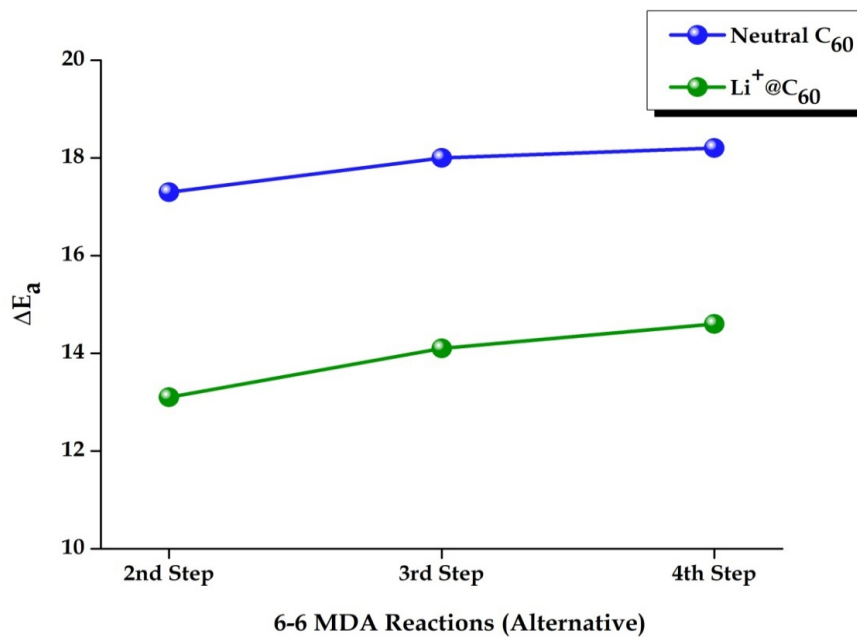

FIGURE 7 Graphical representation of $[?]E_a$ on varying the steps of MDA reactions associated with 6-6 bonds in 'Alternative' approach for both neutral C_{60} and $Li^+@C_{60}$.